

Genome-wide analysis of the response to protein glycosylation deficiency in yeast

Paul J. Cullen^{1,2}, Rufeng Xu-Friedman², Jeffrey Delrow³ & George F. Sprague¹

¹Institute of Molecular Biology, University of Oregon, Eugene, OR, USA; ²Department of Biological Sciences, State University at Buffalo, Buffalo, NY, USA; and ³Genomics Resource, Fred Hutchinson Cancer Research Center Seattle, Washington, DC, USA

Correspondence: Paul J. Cullen, Institute of Molecular Biology, University of Oregon, Eugene OR 97403-1229, USA. e-mail: pjcullen@buffalo.edu

Present address: Rufeng Xu-Friedman, Frontier Science and Technology Research Foundation 4033 Maple Rd, Amherst, NY 14226, USA.

Received 28 February 2006; revised 12 April 2006; accepted 13 April 2006.

doi:10.1111/j.1567-1364.2006.00120.x

Editor: Andrew Alspaugh

Keywords

MAP kinase; signaling; filamentous growth; cell wall.

Abstract

Protein modification by glycosylation occurs through an essential biochemical pathway that produces mannosyl side chain substrates, which are covalently attached to proteins in the endoplasmic reticulum. We used DNA microarray analysis to characterize the cellular response to a conditional defect (*pmi40-101*) in the protein glycosylation pathway. Expression profiles were obtained from DNA microarrays containing essentially every gene from *Saccharomyces cerevisiae*. We validated the microarray analysis by examining the expression patterns of induced genes using transcriptional *lacZ* fusions. The major class of genes differentially expressed in the glycosylation mutant overlapped significantly with that of a starvation response and included those required for gluconeogenesis, the tricarboxylic acid and glyoxylate cycles, and protein and amino acid biosynthesis. Two mitogen-activated protein (MAP) kinase pathways were also activated in the mutant, the filamentous growth and protein kinase C pathways. Taken together, our results suggest that a checkpoint is activated in response to a protein glycosylation defect, allowing the cell to mount an adaptive response by the activation of multiple MAP kinase pathways.



Introduction

Glycosylation of proteins by mannose moiety side chain addition is a posttranslational modification that occurs in the endoplasmic reticulum and Golgi. The pathway responsible for producing these side chains and transferring them to target proteins is conserved throughout eukaryotes. Protein glycosylation is important for protein function (Spiro, 2002), protein folding (Ng *et al.*, 2000), regulated secretion (Scheffele and Fullekrug, 2000), and protein localization (Ohnishi *et al.*, 2003; Watanabe *et al.*, 2004). In addition, carbohydrate moieties of glycoproteins are structurally diverse, imparting specific biological information and regulation onto their cognate proteins.

A change in the rate of protein glycosylation causes several characterized responses, the best studied of which is the unfolded protein response (UPR; Chapman *et al.*, 1998). In addition, defects in protein glycosylation influence secretion (Travers *et al.*, 2000), cell integrity (Lee and Elion, 1999; Cullen *et al.*, 2000), and the activation of cellular signaling pathways (Cullen *et al.*, 2000). How a cell responds to a change in the glycosylation rate is not fully understood, but

presumably the response results from communication between internal cellular signaling networks. Several genomic studies have been employed to characterize the response of cells to abrogation of one aspect of protein glycosylation, N-linked glycosylation, using the inhibitor tunicamycin (Travers *et al.*, 2000; Lecca *et al.*, 2004) or analyzing mutants partially defective for N-linked glycosylation (Klebl *et al.*, 2001).

We previously isolated partial loss-of-function mutants defective in protein glycosylation in a genetic screen for altered expression of a mitogen-activated protein (MAP) kinase pathway-dependent reporter (Cullen *et al.*, 2000). We also demonstrated that in such mutants activation of the MAP kinase pathway is required for viability, indicating that a defect in glycosylation leads to a compensatory cellular response (Cullen *et al.*, 2000). One of the mutants we identified was defective in the *PMI40* gene, which is required for the first committed step of protein glycosylation, the conversion of fructose 6-phosphate to mannose 6-phosphate (Smith *et al.*, 1992). In the present study, we confirm and extend these studies by examining the glycosylation defect using a partial loss-of-function allele of *PMI40*, called

	F E M S Y R	1 2 0		Dispatch: 8.6.06	Journal: FEMS YR	CE: Guna
	Journal Name	Manuscript No.		Author Received:	No. of pages: 10	TE: Sarvan/Suresh

pmi40-101 (Cullen *et al.*, 2000). Expression profiling generated from this study demonstrates that genes encoding structural proteins of two MAP kinase pathways are induced in response to a glycosylation defect. Our data also show that cells defective for glycosylation exhibit a starvation-like response and show growth inhibition. Taken together, our results provide evidence for a checkpoint that is sensitive to the changes in the flux of protein glycosylation in the cell.

Materials and methods

Strains, plasmids, and microbiological techniques

The yeast strains used in this study are listed in Table 1. Integrated green fluorescent protein (GFP) fusions were made by PCR-based methods using plasmids provided by J. Pringle (University of North Carolina; Longtine *et al.*, 1998). Gene disruptions and integrated promoter and protein fusions were confirmed by PCR analysis and by phenotype. GFP-tagged fusion proteins used in this study were functional as assessed by FUS1 reporter expression, invasive growth phenotypes, and viability of the *pmi40-101* mutant. Yeast and bacterial strains were propagated using standard methods (Rose *et al.*, 1990). Yeast peptone dextrose (YPD) and synthetic complete dextrose (SCD) media have been described (Rose *et al.*, 1990). Yeast transformations were performed as described (Gietz *et al.*, 1995). Bacterial transformations, bacterial DNA preparations and plasmid constructions were performed by standard methods (Sambrook *et al.*, 1989). Strains harboring the *pmi40-101* allele were maintained on medium containing 50 mM mannose unless otherwise stated.

Inductions and RNA isolation

Strain *pmi40-101* (1436-13) was grown to stationary phase in YPD medium plus 50 mM mannose. Cells were harvested by centrifugation, washed twice in YPD, and resuspended in YPD (OD 0.5) or YPD plus 50 mM mannose (OD 0.2) medium prewarmed to 30 °C. Cells were incubated at 30 °C until the culture reached OD 0.8 (*c.* 4 h), at which point cells were harvested by centrifugation and stored at -80 °C. RNA was extracted from cells using hot acid phenol extrac-

Table 1. Yeast strains used in this study

Strain	Genotype	Reference
1436	Wild type	Cullen <i>et al.</i> (2000)
1436-13	<i>ste4 pmi40-101</i>	Cullen <i>et al.</i> (2000)
1004	<i>ste4 pmi40-101 ssk1 HOG1-GFP::KanMX6</i>	This study
1006	Σ 1278b <i>ssk1 HOG1-GFP::KanMX6</i>	This study

tion followed by passage over an RNeasy Maxi column (Qiagen, Valencia, CA). Exogenous mannose is not thought to influence the growth rate of wild-type cells (Pitkanen *et al.*, 2004).

Expression analysis

Expression profiles were obtained from microarray analysis performed at the Fred Hutchinson Cancer Research Center. Microarray construction, target labeling and hybridization protocols were performed as described (Fazio *et al.*, 2001). Microarrays were constructed by employing a set of *c.* 6200 ORF-specific PCR primer pairs (Research Genetics, Huntsville, AL). Individual PCR products were verified as unique via gel electrophoresis, purified, and mechanically 'spotted' onto polylysine-coated microscope slides using an Omni-Grid high-precision robotic gridded (GeneMachines, San Carlo, CA). cDNA targets were generated using a standard amino-allyl labeling protocol, where 30 µg each of 'experimental' and 'reference' total RNA was coupled to either Cy3 or Cy5 fluorophores. Targets were cohybridized to microarrays for 16 h at 63 °C and sequentially washed at room temperature in 1 × SSC and 0.03% sodium dodecyl sulfate (SDS) for 2 min, 1 × SSC for 2 min, 0.2 × SSC with agitation for 20 min, and 0.05 × SSC with agitation for 10 min. Arrays were immediately centrifuged until dry and scanned using a GenePix 4000 scanner (Axon Instruments, Union City, CA). Image analysis was performed using GenePix Pro 3.0.

Statistical analysis of the microarray data

For each array, background-subtracted spot intensities (red channel and green channel) were filtered and removed from further analysis if the spot intensity did not exceed 3 SD above the background signal in at least one channel. Red/green ratios were natural log transformed, and a logical regression normalization strategy ($f=0.67$) was applied using S-Plus (MathSoft, Cambridge, MA) to correct for intra-array intensity-dependent ratio bias. Sample comparisons were independently replicated six times, each from a separate cell culture. Pairwise comparisons were made using CyberT (Baldi and Long, 2001) using a default window size of 101 and a confidence value of 6. Significance was determined by ranking the Bayesian *P*-values and using a false discovery rate methodology (FDR=0.05) to account for multiple testing. A series of three 'same vs. same' hybridizations was performed using independent cultures, and the spot-level averaged normalized ratios were subtracted from the averaged normalized ratio of the six experimental replicates to correct for residual dye effects. A fold-change threshold of ≥ 1.5 was applied as an additional significance criterion, based in part on the expression pattern of known targets. This threshold was derived from ratios taken from the 'same vs. same' observations, where

1 the threshold was set at four times the average SD value. Accordingly, any ORFs with a *P*-value that met the FDR = 0.05 criterion and where the normalized ratio was ≥ 1.5 were identified as differentially expressed. Heat maps were generated using the Eisen Cluster/Tree View Package (Eisen *et al.*, 1998).

Validation of microarray data by transcriptional fusions

10 Transcriptional (*lacZ*) fusions were constructed to a subset of genes that showed differential expression by DNA microarray analysis. Plasmid V84 and plasmids containing filamentous growth pathway targets fused to *lacZ* for KSS1 (p2987), PGU1 (p2985), SVS1 (p3017) and YLR042c (p2988) were provided by C. Boone (University of Toronto; Roberts *et al.*, 2000). Other gene fusions have also been described (Cullen *et al.*, 2000, 2004). Reporter plasmids were transformed into the *pmi40-101* strain, and β -galactosidase assays were performed in induced [yeast extract-peptone-dextrose (YEPD) medium] and uninduced (YEPD+50 mM mannose) conditions. Cells harboring the *MSB2-lacZ* reporter were assessed over multiple time points (2 h, 4 h, 8 h, and 16 h). Assays were performed from cell extracts derived from three separate trials, and the average of the values were expressed in Miller Units as previously described (Cullen *et al.*, 2000). The resultant microarray data have been made available on the SGD Website (<http://www.yeastgenome.org/>).

Protein localization

15 Hog1-GFP localization was performed using a C-terminal Hog1-GFP fusion integrated at the *HOG1* locus into a *pmi40-101 ssk1* strain (1004) or an *ssk1* strain in the filamentous background (1006). Cells were visualized by microscopy at $\times 100$ using a fluorescein isothiocyanate (FITC) filter. Nuclei were visualized by 4,6-diamidino-2-phenylindole (DAPI) staining as previously described (Rose *et al.*, 1990).

Microscopy

20 Differential-interference-contrast (DIC) and fluorescence microscopy using UV and FITC filter sets were performed using an Axioplan 2 microscope (Zeiss, Jena, Germany), a black and white Orca II digital camera (Hamamatsu, San Jose, CA), and the Openlab software program (Improvision, Coventry, UK).

Results and discussion

25 We turned to DNA microarray analysis (DeRisi *et al.*, 1997) to better understand the cellular response to a protein

glycosylation defect and to define the signaling pathways activated under this condition. We focused on the *pmi40-101* mutant (Cullen *et al.*, 2000), which exhibits a conditional glycosylation defect: when grown in the presence of mannose, no glycosylation defect is apparent; when grown in the absence of mannose, a glycosylation defect is evident (Smith *et al.*, 1992; Cullen *et al.*, 2000). Spotted cDNA microarrays (DeRisi *et al.*, 1997; Lashkari *et al.*, 1997) representing $>96\%$ of all yeast ORFs were used to monitor the changes in expression in the inducible glycosylation defect in the *pmi40-101* mutant.

Expression analysis of a glycosylation mutant

15 cDNA sequences were prepared from the *pmi40-101* mutant incubated in medium containing mannose, and compared to those obtained from incubation in medium lacking mannose at a 4 h time point, at which time significant MAP kinase activation occurs (data not shown). Six independent comparisons were performed, and most genes that had differential expression showed a highly correlative pattern between replicates. To validate the expression data, a statistical analysis was used in which variable signals were flagged and removed from the dataset. Significance was determined by a Bayesian method derived for microarray analysis (CyberT; Baldi and Long, 2001) and using an FDR methodology to account for multiple testing. Control hybridizations were performed and subtracted from the averaged normalized ratio of the experimental replicates to account for by biases. We established a fold-change threshold of ≥ 1.5 as an additional significance criterion, based in part on the expression pattern of known induced targets. Only ORFs with a *P*-value that met the significance criterion and where the normalized ratio was ≥ 1.5 were identified as differentially expressed. The results of this analysis indicate differential induction of *c.* 740 ORFs, and repression of *c.* 440 ORFs was observed in the *pmi40-101* mutant.

20 To validate the DNA microarray data, we analyzed a series of transcriptional fusions to a subset of the promoters that showed differential expression. β -Galactosidase assays were performed using promoter fusions carried in the *pmi40-101* strain. All promoter fusions tested (*SVS1*, *MSB2*, *FUS1*, *YLR042c*, *KSS1*, *FgTy1*, *FRE*, and *PGU1*) showed a >2 -fold induction of gene expression in mannose-limiting media (Fig. 1), indicating a strong correlation with the expression profile data. Databases containing annotated yeast genes (SGD, <http://www.yeastgenome.org/>) were used to classify the differentially expressed genes in the *pmi40-101* mutant. Differentially induced gene sets fell into distinct functional classes, which were analyzed and compared with other genome-wide expression profiles. These results are summarized below.

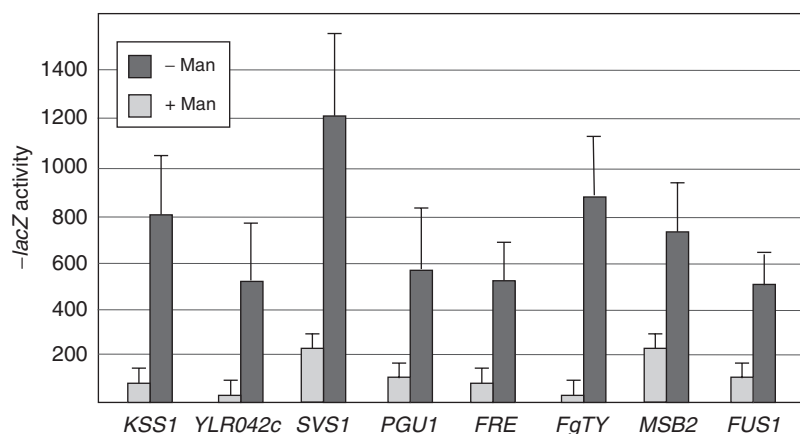


Fig. 1. Verification of a subset of microarray targets using transcriptional reporter gene fusions. The *pmi40-101* mutant (strain 1436-13) containing *lacZ* fusions to the denoted genes was incubated for 4 h in medium containing (light rectangles) or lacking (dark rectangles) 50 mM mannose. β -Galactosidase assays were performed as described. The average of two independent experiments is shown.

Unfolded protein response

Altered glycosylation of proteins in the endoplasmic reticulum triggers the UPR, resulting in the induction of an intracellular signaling pathway that functions to promote protein folding and degrade misfolded proteins (Chapman *et al.*, 1998). Expression profiles using drug treatments that block N-linked glycosylation (Travers *et al.*, 2000) or in mutants partially defective for N-linked glycosylation (Klebl *et al.*, 2001) have identified a number of genes whose products contribute to the UPR. The expression profile of the *pmi40-101* mutant showed that most of the genes that play a role in the UPR were induced. These genes include *HAC1*, which encodes the transcription factor (Mori *et al.*, 2000), and a number of its targets, *INO1*, *ERO1*, *KAR2*, *PDI1*, *OPI3*, *YET1*, and *DER1* (Table 2). In addition, genes encoding proteins that promote protein folding were differentially induced, including *LHS1*, *MPD1*, *EUG1*, and *FKB2* (Fig. S1). Thus, as expected in a mutant defective for protein glycosylation, transcriptional targets of the UPR were induced.

Environmental stress response (ESR)

The ESR in yeast is a general stress response resulting in the coordinated activation of independent stress-responsive pathways (Gasch *et al.*, 2000). We considered the possibility that a defect in glycosylation induces this general stress response. Comparison of genes induced >2-fold in the *pmi40-101* mutant with those induced >2-fold in the ESR showed only a 14% overlap for characterized ORFs (Fig. S2). Most of the overlapping genes encode proteins that play a role in the heat shock response (*HSP42*, *SSE2*, and *HSP104*), protein degradation (*PRB1* and *PMC1*), and nutrition (*GLK1*, *YDR516c*, *PDE1*, *GLC3*, and *NTH1*). Therefore, although some ESR genes are induced in the *pmi40-101* mutant, the transcriptional response was largely distinct from the ESR.

Nutritional pathways

A large subset of the differentially expressed genes in the *pmi40-101* mutant are differentially expressed during the diauxic shift, which represents entry into stationary phase (DeRisi *et al.*, 1997). In particular, the expression of genes required for gluconeogenesis was induced in the *pmi40-101* mutant, including *Cat8*, which encodes a transcription factor for gluconeogenesis (Fig. S3) and the *Cat8* targets *PCK1*, *MDH2*, *IDP2*, *JEN1*, and *SFC1* (Table 2). Genes that are required for hexose transport, trehalose, glycogen and glycerol metabolism, the glyoxylate cycle, ATP synthesis and poor carbon source utilization also showed differential induction (Table 2 and Fig. S3). Likewise, some genes known to be controlled by glucose repression (e.g. *INO1*, *PHO89*, *AMS1*, *PCK1*, *MDH2*, *IDP2*, *ACS1*, *HXT2*, *HXT16*, and *ADR1*) were induced in the *pmi40-101* mutant (Fig. S3).

The gene expression profile in the *pmi40-101* mutant differs from that of the diauxic shift in several ways. Most genes encoding citric acid cycle enzymes are not affected in the *pmi40-101* mutant (13/14), although they are reported to be induced during the diauxic shift (DeRisi *et al.*, 1997). Similarly, the genes required for respiration are not induced in the *pmi40-101* mutant but are induced during the diauxic shift (DeRisi *et al.*, 1997). Indeed, genes encoding mitochondrial ribosomal proteins, mitochondrial protein import machinery and proteins known to be associated with respiration were modestly repressed in the *pmi40-101* mutant (data not shown). On the other hand, genes that encode components of the protein glycosylation pathway itself and genes required for recycling mannosyl moieties (Table 2) were induced in the *pmi40-101* mutant but not in the diauxic shift.

Upon nutrient limitation, coordinate repression of ribosome biosynthetic genes occurs (Warner, 1999; Raught *et al.*, 2001). We also observed that the expression of ribosome biosynthetic genes was modestly repressed in the *pmi40-101* mutant (Fig. S3). The only exception was *MPR8*, which

Q7 Table 2. Microarray analysis of UPR, nutrition, cell cycle, and glycosylation-related genes differentially expressed in the *pmi40-101* mutant

Gene name	Fold change	P-value	Process/function
UPR			
<i>INO1</i>	10.7	< 0.001	Inositol biosynthesis; inositol-1-phosphate synthase
<i>ERO1</i>	4.5	< 0.001	Protein folding; disulfide bond formation in the endoplasmic reticulum
<i>KAR2</i>	3.0	< 0.001	Secretion; BiP homolog; endoplasmic reticulum protein translocation
<i>HAC1</i>	3.0	0.038	Transcription factor for UPR
<i>PDI1</i>	2.8	< 0.001	Protein folding; protein disulfide isomerase
<i>OPB3</i>	2.2	< 0.001	Phospholipid metabolism; phospholipid synthase
<i>YET1</i>	2.2	< 0.001	Endoplasmic reticulum 25 kDa transmembrane protein
<i>DER1</i>	2.1	< 0.001	Protein degradation, endoplasmic reticulum
Gluconeogenesis			
<i>PCK1</i>	5.9	< 0.001	Phosphoenolpyruvate carboxykinase; Cat8 target
<i>MDH2</i>	3.1	< 0.001	Malate dehydrogenase; Cat8 target
<i>LSC2</i>	2.5	< 0.001	Succinyl-CoA ligase
<i>GLK1</i>	2.3	0.001	Glycolysis; glucokinase
<i>CIT2</i>	2.3	< 0.001	Glyoxylate cycle; peroxisomal citrate synthase
<i>NTH1</i>	2.2	< 0.001	Trehalose metabolism; α -trehalase
<i>SFC1</i>	2.1	< 0.001	Transport; succinate-fumarate carrier; Cat8 target
<i>IDP2</i>	2.1	< 0.001	Isocitrate dehydrogenase; Cat8 target
Hexose permease			
<i>HXT2</i>	3.6	< 0.001	High-affinity glucose transporter
<i>HXT13</i>	2.3	0.006	Hexose transporter
<i>HXT16</i>	2.1	< 0.001	Hexose transporter
Glycerol metabolism			
<i>GUT2</i>	3.4	< 0.001	Glycerol-3-phosphate dehydrogenase, mitochondrial
<i>RHR2</i>	2.2	< 0.001	DL-glycerol-3-phosphatase
<i>HOR2</i>	2.2	< 0.001	DL-glycerol-3-phosphatase
ATP synthesis			
<i>STF1</i>	3.4	< 0.001	ATPase stabilizing factor
<i>STF2</i>	2.9	0.001	ATPase stabilizing factor
<i>ATP3</i>	2.0	< 0.001	Mitochondrial F1FO ATP synthase subunit
Amino acid biosynthesis			
<i>ARG3</i>	-2.0	< 0.001	Arginine biosynthesis; ornithine carbamoyltransferase
<i>CPA2</i>	-2.0	< 0.001	Glutamate metabolism; carbamyl phosphate synthetase
<i>HOM2</i>	-2.1	< 0.001	Threonine and methionine biosynthesis
<i>SAM3</i>	-2.1	< 0.001	Transport, amino acid; S-adenosylmethionine permease
<i>BAT2</i>	-2.4	< 0.001	Branched-chain amino acid biosynthesis; transaminase
<i>ARG1</i>	-3.0	< 0.001	Arginine biosynthesis; arginosuccinate synthetase
Cell cycle			
<i>PCL1</i>	3.3	< 0.001	G1/S cyclin
<i>CLN1</i>	1.5	0.002	G1/S cyclin
<i>CLN2</i>	1.9	< 0.001	G1/S cyclin
<i>CLN3</i>	1.5	0.001	G1/S cyclin
<i>SIM1</i>	2.4	< 0.001	Cytoskeleton organization, control of DNA replication
<i>HSL1</i>	2.3	< 0.001	G2/M; negative regulator of Swe1 kinase
<i>PCL7</i>	2.0	< 0.001	Glycogen biosynthesis; CDK regulator
<i>CLB2</i>	-2.1	< 0.001	G2/M cyclin
<i>CLB1</i>	-3.5	< 0.001	G2/M cyclin
Glycosylation			
<i>AMS1</i>	5.2	< 0.001	Cell wall catabolism; vacuolar α -mannosidase
<i>KTR2</i>	4.3	< 0.001	Protein glycosylation; putative mannosyltransferase

Results are presented as fold changes in mRNA levels (≥ 2 and ≤ -2). Gene descriptions are from the *Saccharomyces* Genome database (<http://www.yeastgenome.org>)

showed induced expression (Fig. S3). This is consistent with previous reports (Yale and Bohnert, 2001; Parveen *et al.*, 2003) indicating a distinct regulatory function for

the protein. Genes involved in amino acid biosynthesis were also repressed in the *pmi40-101* mutant (Table 2 and Fig. S3).

Cell cycle

Cell growth and the cell cycle are coupled processes (Tapon *et al.*, 2001). Many genes are cell cycle regulated, and their differential expression by DNA microarray analysis can be used to pinpoint changes in cell cycle progression (Futcher, 2000). We examined the expression profile of the *pmi40-101* mutant for such a bias and found differential induction of G₁-associated transcripts, including the G₁ cyclins (Levine *et al.*, 1995) encoded by the *CLN1*, *CLN2* and *CLN3* genes, and the gene encoding the Pho85 G₁ cyclin *PCL1* (Table 2 and Fig. S1). Genes that control entry into the G₂ phase of the cell cycle (Yeong *et al.*, 2001) were repressed, including the cyclins *CLB1* and *CLB2* (Table 2 and Fig. S1). Delay in the G₁ phase of the cell cycle is consistent with entry into stationary phase (Reinders *et al.*, 1998) and with the slow growth defect and higher percentage of round, unbudded cells observed in the *pmi40-101* mutant (data not shown). G₁ delay is also consistent with the G₁ arrest observed in cells containing misfolded proteins (Trotter *et al.*, 2001). Delay in the G₁ phase of the cell cycle indicates that a cell cycle checkpoint is initiated in the mutant in response to a glycosylation defect.

Defects in protein glycosylation activate the protein kinase C (PKC) and filamentous growth MAP kinase pathways

Activation of MAP kinase pathways can occur in response to a wide variety of cellular stresses. We examined the expression of known MAP kinase pathway targets to characterize the signaling response initiated in the *pmi40-101* mutant. Comparison of the expression profile of the *pmi40-101* mutant with targets of the cell wall integrity pathway (or PKC pathway) (Jung and Levin, 1999) revealed that 72% (18/25) of known PKC targets were induced in the *pmi40-101* mutant (Table 3; Fig. S4). In addition, genes that encode components of that pathway, including the MAP kinase Mpk1 (Slt2), and transcription factor, Rlm1 (Jung *et al.*, 2002), were modestly induced in the *pmi40-101* mutant (Fig. S4).

Activation of the PKC pathway can occur in response to integrity defects in the cell wall (Levin *et al.*, 1994; Kamada *et al.*, 1995). Comparison of the expression profile of the *pmi40-101* mutant with an expression profile derived from cells defective for 1,3- β -glucan synthase (*fks1*; Terashima *et al.*, 2000) showed a striking overlap: 91% (20/22) of the genes induced in an *fks1* mutant were also induced in the *pmi40-101* mutant (Fig. S4). Most of these genes also contain Rlm1-binding sites in their promoter regions (Terashima *et al.*, 2000). The induced cell wall genes include those that encode cell wall constituents such as chitin synthases (*CHS1*, *CHS3*, and *CHS7*) and genes that contribute to chitin biosynthesis (*CSI2* and *GFA1*). The expression of several

other genes known to influence cell wall biosynthesis, but not known Rlm1 targets, was induced in the *pmi40-101* mutant, including *SCW10*, which encodes a cell wall glucanase, and *KRE11*, which encodes a regulator of β -1,6-glucan synthesis (Fig. S4). Activation of the PKC pathway in response to a glycosylation defect is consistent with the increased sensitivity of the *pmi40-101* mutant to cell wall-perturbing agents (Cullen *et al.*, 2000), with the previously reported induction of *FKS2* (*GSC2*) expression observed in protein glycosylation mutants (Lee and Elion, 1999), and with the requirement for the PKC pathway for viability of glycosylation mutants (Cullen *et al.*, 2000). As general cell wall defects resulting from hypoglycosylation of cell wall mannoproteins (Osmond *et al.*, 1999), and defects in β -1,6-glucan synthesis (Chavan *et al.*, 2003), induce similar responses, the data indicate that a defect in protein glycosylation causes a cell wall defect, which in turn triggers a PKC pathway-dependent response to maintain cell integrity.

We previously showed that a second MAP kinase pathway, the filamentous growth pathway, is activated in response to a protein glycosylation defect and is required for viability under this condition (Cullen *et al.*, 2000). The expression profile of the *pmi40-101* mutant confirmed that targets of the filamentous growth pathway (Roberts *et al.*, 2000), including *SVS1*, *YLR042c*, and *PGU1*, were induced in the *pmi40-101* mutant. One exception was the *FLO11* gene, which is a known filamentous growth pathway target (Rupp *et al.*, 1999) that was downregulated in the *pmi40-101* mutant (Fig. S5). The *FLO11* promoter is complex (Rupp *et al.*, 1999) and contains *cis*-elements on which multiple signaling pathways converge; thus, its regulation in this instance may reflect the combined influence of multiple pathways. Genes that encode components of the filamentous growth pathway, including *MSB2* and *KSS1* (Table 3) (Cullen *et al.*, 2004), were also induced in the *pmi40-101* mutant. Filamentous growth is known to occur in response to nutrient depletion (Gimeno *et al.*, 1992; Cullen and Sprague, 2000). Since the expression profile of the *pmi40-101* mutant indicates that the cells suffer nutritional stress, it is possible that this condition contributes to activation of the filamentous growth pathway.

Filamentous growth pathway activation is distinct from high osmolarity glycerol response (HOG) pathway activation

We determined if targets of a third MAP kinase pathway, the HOG pathway, were induced in the *pmi40-101* mutant. Transcriptional targets of the HOG pathway, including *GPD1*, *CTT1*, *GPH1*, *HOR2*, *SIP18*, *GRE1*, *PGM2*, *STL1*, and *ALD6* (Posas *et al.*, 2000; O'Rourke and Herskowitz, 2004), were not induced in the *pmi40-101* mutant (Table 3), even at time points at which HOG pathway activation is

Table 3. Microarray analysis of MAP kinase targets differentially expressed in the *pmi40-101* mutant

Gene name	Fold change	P-value	Process/function
PKC			
<i>PRM5*</i>	12.9	< 0.001	Pheromone-regulated protein, induced by PKC
<i>YLR194C</i>	8.2	< 0.001	Unknown
<i>PIR3</i>	4.5	< 0.001	Cell wall organization and biogenesis
<i>FKS2</i>	4.3	< 0.001	Cell wall biogenesis; 1,3- β -D-glucan synthase subunit
<i>CRH1</i>	4.1	< 0.001	Cell wall biogenesis (putative); cell wall protein
<i>PST1*</i>	3.2	< 0.001	Secreted by regenerating protoplasts
<i>HSP150</i>	2.9	< 0.001	Heat shock response; secreted glycoprotein of heat shock protein (HSP) family
<i>DFG5</i>	2.7	< 0.001	Pseudohyphal growth
<i>CIS3</i>	2.6	< 0.001	Unknown
<i>SED1</i>	2.4	< 0.001	Cell surface glycoprotein
<i>CHS3</i>	2.2	< 0.001	Cell wall biogenesis; chitin synthase III
<i>SLT2</i>	2.1	< 0.001	MAP kinase for PKC pathway
Filamentous growth			
<i>SVS1</i>	11.4	< 0.001	Vanadate resistance
<i>RTA1</i>	5.6	< 0.001	7-Aminocholesterol resistance
<i>YLR042C</i>	5.3	< 0.001	Unknown
<i>KTR2</i>	4.3	< 0.001	Protein glycosylation; putative mannosyltransferase
<i>YLR414C</i>	3.2	< 0.001	Unknown
<i>YPS1</i>	3.1	< 0.001	Protein processing; GPI-anchored aspartic protease
<i>MSB2</i>	2.7	< 0.001	Filamentous growth pathway; cell surface component
<i>MPT5</i>	2.2	< 0.001	Cell wall organization and biogenesis
<i>YOR248W</i>	2.2	< 0.001	Unknown
<i>KSS1</i>	2.1	< 0.001	MAP kinase for the filamentous growth pathway
<i>DDR48</i>	2.1	< 0.001	Induced by DNA damage, heat shock, or osmotic stress
<i>WSC2</i>	2.0	< 0.001	Cell wall biogenesis; α -1,4-glucan-glucosidase
<i>FLO11</i>	-9.6	< 0.001	Flocculation, invasive growth; regulated by the MAP kinase and cAMP pathways
HOG			
<i>YDL223C</i>	2.3	< 0.001	Cellular morphogenesis
<i>RHR2</i>	2.2	< 0.001	Glycerol metabolism; DL-glycerol-3-phosphatase
<i>HOR2</i>	2.2	< 0.001	Glycerol metabolism; DL-glycerol-3-phosphatase

Results are presented as fold changes in mRNA levels (≥ 2 and ≤ -2). Gene descriptions are from the *Saccharomyces* Genome database (<http://www.yeastgenome.org>).

*Target of both PKC and filamentous growth pathways.

GPI, glycosylphosphatidylinositol.

reported to be maximal (data not shown). Only three HOG pathway targets were significantly induced: *YDL233c*, *RHR2*, and *HOR2* (Table 3). Moreover, expression of the gene encoding the HOG pathway MAP kinase, *HOG1*, was not induced (Fig. S5).

Sho1 is an upstream component of both the filamentous growth and HOG pathways (Cullen *et al.*, 2004). The DNA microarray analysis suggests that Sho1 activation is restricted to the filamentous growth pathway in the glycosylation mutant. This hypothesis is supported by expression analysis of cells undergoing filamentous growth (Madhani *et al.*, 1999; Roberts *et al.*, 2000) and by a report indicating that the HOG and PKC pathways function antagonistically (Garcia-Rodriguez *et al.*, 2000). We determined whether Sho1 functions specifically in the filamentous growth pathway during a glycosylation defect. We used the nuclear localization of the HOG pathway MAP kinase Hog1 (Ferrigno *et al.*, 1998; Reiser *et al.*, 2000) to measure Sho1

activity in the HOG pathway. An integrated and functional Hog1-GFP fusion in the *pmi40-101* mutant lacking the Sln1 branch of the HOG pathway (Posas and Saito, 1998) (*ssk1*) showed predominantly cytoplasmic localization of Hog1-GFP throughout a culture growth cycle in medium lacking mannose (Figs 2a and b). Addition of salt (0.9 M NaCl) caused rapid nuclear localization of Hog1-GFP in >90% of cells (Figs 2a and b). We also examined the specificity of Sho1 function in response to filamentous growth pathway activation. We found that the HOG pathway is not activated during filamentation in the Σ 1278b background based on cytoplasmic localization of Hog1-GFP in *ssk1* strains in glucose-limited medium (Fig. 2c). Therefore, in the two contexts in which Sho1 functions in the filamentous growth pathway, its activity appears to be restricted to that pathway.

Although Sho1 activity in the filamentous growth pathway does not trigger HOG pathway activation, Sho1 retains

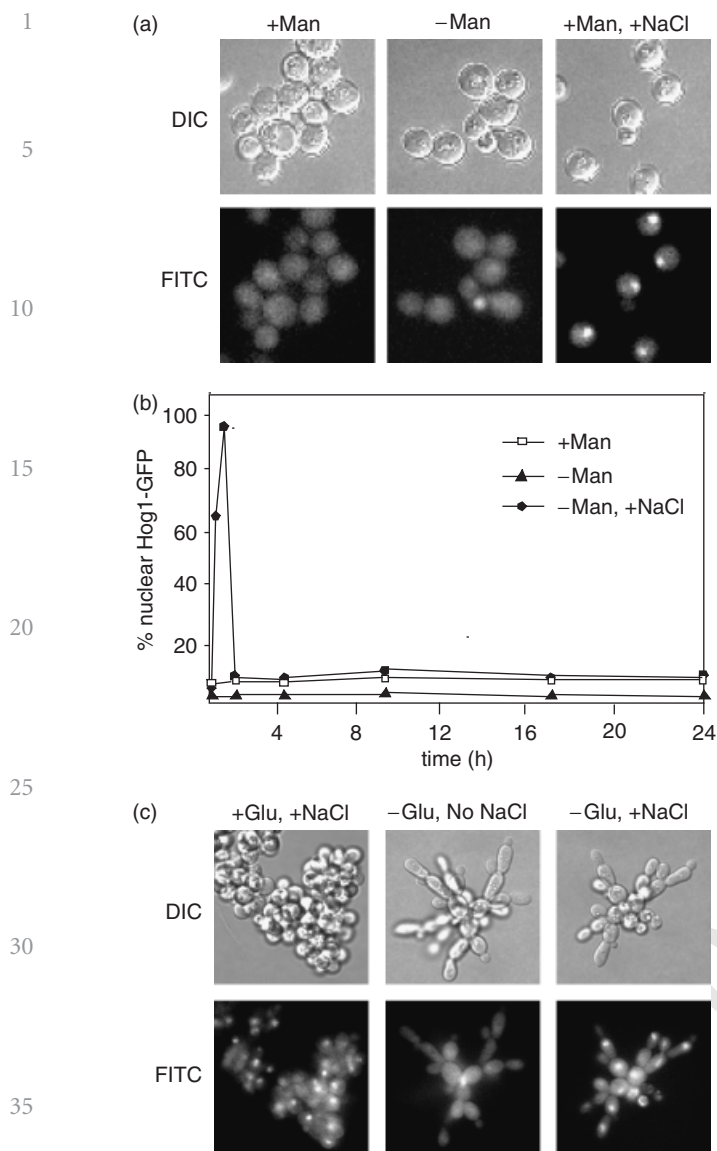


Fig. 2. Sho1 activation in response to a glycosylation defect or during filamentous growth does not activate the HOG pathway. (a) The *pmi40-101* mutant containing *ssk1* and an integrated *Hog1-GFP* fusion (strain 1004) was grown in medium containing mannose (+Man), lacking mannose (-Man) or lacking mannose and containing 0.9 M NaCl (-Man, +NaCl). Cells were examined by differential interference contrast (DIC) or fluorescence (FITC) microscopy at $\times 1000$. Bar, 10 μm . (b) Graph of nuclear *Hog1-GFP* over a culture growth cycle. The strain in (a) was grown in media containing mannose (white squares, +Man), lacking mannose (filled triangles, -Man), or lacking mannose and containing 0.9 M NaCl (filled circles, -Man, +NaCl) over a culture growth cycle and periodically assayed for nuclear *Hog1-GFP* localization. (c) Filamentous $\Sigma 1278b$ cells lacking *ssk1* and containing *Hog1-GFP* (strain 1006) were grown on minimal semisolid agar media containing or lacking glucose (Glu) for 24 h at 30 $^{\circ}\text{C}$. A coverslip was added directly to the plate and cells were examined. Where indicated, NaCl (final 200 mM) was also added to the plate. Cells were examined by DIC or fluorescence (FITC) microscopy at $\times 1000$. Bar, 10 μm .

the capacity to function in the HOG pathway under conditions in which the filamentous growth pathway is active. Specifically, addition of salt to *pmi40-101 ssk1 HOG1-GFP* cells in medium lacking mannose (data not shown), or to *ssk1 HOG1-GFP* cells undergoing filamentous growth, caused rapid nuclear localization of *Hog1-GFP* (Fig. 2c). Therefore, Sho1 function in the filamentous growth pathway does not preclude its ability to activate the HOG pathway.

In summary, we have identified a large number of genes that are differentially expressed in response to a defect in protein glycosylation. An important subset of these are transcriptional targets of two MAP kinase pathways, indicating that one cellular response to glycosylation deficiency is MAP kinase pathway activation. This response may be a common theme in intracellular regulation in eukaryotic cells.

Acknowledgements

This work was supported by a research grant from the US Public Health Service (GM-30027 for G.F.S.) and a post-doctoral fellowship from the American Heart Association (AHA120635Z for P.C.). We thank Charlie Boone and John Pringle for plasmids, and Marc Dorfman for assistance with *Hog1-GFP* localization.

References

- Baldi P & Long AD (2001) A Bayesian framework for the analysis of microarray expression data: regularized *t*-test and statistical inferences of gene changes. *Bioinformatics* **17**: 509–519.
- Chapman R, Sidrauski C & Walter P (1998) Intracellular signaling from the endoplasmic reticulum to the nucleus. *Annu Rev Cell Dev Biol* **14**: 459–485.
- Chavan M, Suzuki T, Rekowicz M & Lennarz W (2003) Genetic, biochemical, and morphological evidence for the involvement of N-glycosylation in biosynthesis of the cell wall beta1,6-glucan of *Saccharomyces cerevisiae*. *Proc Natl Acad Sci USA* **100**: 15381–15386.
- Cullen PJ & Sprague GF Jr (2000) Glucose depletion causes haploid invasive growth in yeast. *Proc Natl Acad Sci USA* **97**: 13619–13624.
- Cullen PJ, Schultz J, Horecka J, Stevenson BJ, Jigami Y & Sprague GF Jr (2000) Defects in protein glycosylation cause SHO1-dependent activation of a STE12 signaling pathway in yeast. *Genetics* **155**: 1005–1018.
- Cullen PJ, Sabbagh W Jr, Graham E, Irick MM, van Olden EK, Neal C, Delrow J, Bardwell L & Sprague GF Jr (2004) A signaling mucin at the head of the Cdc42- and MAPK-dependent filamentous growth pathway in yeast. *Genes Dev* **18**: 1695–1708.

- 1 DeRisi JL, Iyer VR & Brown PO (1997) Exploring the metabolic and genetic control of gene expression on a genomic scale. *Science* **278**: 680–686.
- 5 Eisen MB, Spellman PT, Brown PO & Botstein D (1998) Cluster analysis and display of genome-wide expression patterns. *Proc Natl Acad Sci USA* **95**: 14863–14868.
- Fazio TG, Kooperberg C, Goldmark JP, Neal C, Basom R, Delrow J & Tsukiyama T (2001) Widespread collaboration of Isw2 and Sin3-Rpd3 chromatin remodeling complexes in transcriptional repression. *Mol Cell Biol* **21**: 6450–6460.
- 10 Ferrigno P, Posas F, Koepf D, Saito H & Silver PA (1998) Regulated nucleo/cytoplasmic exchange of HOG1 MAPK requires the importin beta homologs NMD5 and XPO1. *EMBO J* **17**: 5606–5614.
- 15 Futcher B (2000) Microarrays and cell cycle transcription in yeast. *Curr Opin Cell Biol* **12**: 710–715.
- Garcia-Rodriguez LJ, Duran A & Roncero C (2000) Calcofluor antifungal action depends on chitin and a functional high-osmolarity glycerol response (HOG) pathway: evidence for a physiological role of the *Saccharomyces cerevisiae* HOG pathway under noninducing conditions. *J Bacteriol* **182**: 2428–2437.
- 20 Gasch AP, Spellman PT, Kao CM, Carmel-Harel O, Eisen MB, Storz G, Botstein D & Brown PO (2000) Genomic expression programs in the response of yeast cells to environmental changes. *Mol Biol Cell* **11**: 4241–4257.
- Gietz RD, Schiestl RH, Willems AR & Woods RA (1995) Studies on the transformation of intact yeast cells by the *liac*/SS-DNA/PEG procedure. *Yeast* **11**: 355–360.
- 30 Gimeno CJ, Ljungdahl PO, Styles CA & Fink GR (1992) Unipolar cell divisions in the yeast *S. cerevisiae* lead to filamentous growth: regulation by starvation and RAS. *Cell* **68**: 1077–1090.
- Jung US & Levin DE (1999) Genome-wide analysis of gene expression regulated by the yeast cell wall integrity signalling pathway. *Mol Microbiol* **34**: 1049–1057.
- 35 Jung US, Sobering AK, Romeo MJ & Levin DE (2002) Regulation of the yeast Rlm1 transcription factor by the Mpk1 cell wall integrity MAP kinase. *Mol Microbiol* **46**: 781–789.
- Kamada Y, Jung US, Piotrowski J & Levin DE (1995) The protein kinase C-activated MAP kinase pathway of *Saccharomyces cerevisiae* mediates a novel aspect of the heat shock response. *Genes Dev* **9**: 1559–1571.
- 40 Klebl B, Kozian D, Leberer E & Kukuruzinska MA (2001) A comprehensive analysis of gene expression profiles in a yeast N-glycosylation mutant. *Biochem Biophys Res Commun* **286**: 714–720.
- 45 Lashkari DA, DeRisi JL, McCusker JH, Namath AF, Gentile C, Hwang SY, Brown PO & Davis RW (1997) Yeast microarrays for genome wide parallel genetic and gene expression analysis. *Proc Natl Acad Sci USA* **94**: 13057–13062.
- 50 Lecca MR, Wagner U, Patrignani A, Berger EG & Hennet T (2004) Genome-wide analysis of the unfolded protein response in fibroblasts from congenital disorders of glycosylation type-I patients. *Faseb J*.
- Lee BN & Elion EA (1999) The MAPKKK Ste11 regulates vegetative growth through a kinase cascade of shared signaling components. *Proc Natl Acad Sci USA* **96**: 12679–12684.
- Levin DE, Bowers B, Chen CY, Kamada Y & Watanabe M (1994) Dissecting the protein kinase C/MAP kinase signalling pathway of *Saccharomyces cerevisiae*. *Cell Mol Biol Res* **40**: 229–239.
- Levine K, Tinkelenberg AH & Cross F (1995) The CLN gene family: central regulators of cell cycle Start in budding yeast. *Prog Cell Cycle Res* **1**: 101–114.
- 10 Longtine MS, McKenzie A III, Demarini DJ, Shah NG, Wach A, Brachat A, Philippsen P & Pringle JR (1998) Additional modules for versatile and economical PCR-based gene deletion and modification in *Saccharomyces cerevisiae*. *Yeast* **14**: 953–961.
- 15 Madhani HD, Galitski T, Lander ES & Fink GR (1999) Effectors of a developmental mitogen-activated protein kinase cascade revealed by expression signatures of signaling mutants. *Proc Natl Acad Sci USA* **96**: 12530–12535.
- Mori K, Ogawa N, Kawahara T, Yanagi H & Yura T (2000) mRNA splicing-mediated C-terminal replacement of transcription factor Hac1p is required for efficient activation of the unfolded protein response. *Proc Natl Acad Sci USA* **97**: 4660–4665.
- 20 Ng DT, Spear ED & Walter P (2000) The unfolded protein response regulates multiple aspects of secretory and membrane protein biogenesis and endoplasmic reticulum quality control. *J Cell Biol* **150**: 77–88.
- O'Rourke SM & Herskowitz I (2004) Unique and redundant roles for HOG MAPK pathway components as revealed by whole-genome expression analysis. *Mol Biol Cell* **15**: 532–542.
- 30 Ohnishi T, Muroi M & Tanamoto K (2003) MD-2 is necessary for the toll-like receptor 4 protein to undergo glycosylation essential for its translocation to the cell surface. *Clin Diagn Lab Immunol* **10**: 405–410.
- Osmond BC, Specht CA & Robbins PW (1999) Chitin synthase III: synthetic lethal mutants and 'stress-related' chitin synthesis that bypasses the CSD3/CHS6 localization pathway. *Proc Natl Acad Sci USA* **96**: 11206–11210.
- 35 Parveen M, Momose Y, Kitagawa E, Kurita S, Kodama O & Iwahashi H (2003) Bioassay of pesticide Lindane using yeast-DNA microarray technology. *Chem-Bio Informatics J* **3**: 12–29.
- 40 Pitkanen JP, Torma A, Alff S, Huopaniemi L, Mattila P & Renkonen R (2004) Excess mannose limits the growth of phosphomannose isomerase PMI40 deletion strain of *Saccharomyces cerevisiae*. *J Biol Chem*.
- 45 Posas F & Saito H (1998) Activation of the yeast SSK2 MAP kinase kinase by the SSK1 two-component response regulator. *EMBO J* **17**: 1385–1394.
- Posas F, Chambers JR, Heyman JA, Hoeffler JP, de Nadal E & Arino J (2000) The transcriptional response of yeast to saline stress. *J Biol Chem* **275**: 17249–17255.
- 50 Raught B, Gingras AC & Sonenberg N (2001) The target of rapamycin (TOR) proteins. *Proc Natl Acad Sci USA* **98**: 7037–7044.

- Reinders A, Burckert N, Boller T, Wiemken A & De Virgilio C (1998) *Saccharomyces cerevisiae* camp-dependent protein kinase controls entry into stationary phase through the Rim15p protein kinase. *Genes Dev* **12**: 2943–2955.
- Reiser V, Salah SM & Ammerer G (2000) Polarized localization of yeast Pbs2 depends on osmopressure, the membrane protein Sho1 and Cdc42. *Nat Cell Biol* **2**: 620–627.
- Roberts CJ, Nelson B, Marton MJ, et al. (2000) Signaling and circuitry of multiple MAPK pathways revealed by a matrix of global gene expression profiles. *Science* **287**: 873–880.
- Rose MD, Winston F & Hieter P (1990) *Methods in Yeast Genetics*. Cold Spring Harbor Laboratory Press, Cold Spring Harbor, NY.
- Rupp S, Summers E, Lo HJ, Madhani H & Fink G (1999) MAP kinase and camp filamentation signaling pathways converge on the unusually large promoter of the yeast FLO11 gene. *EMBO J* **18**: 1257–1269.
- Sambrook J, Fritsch EF & Maniatis T (1989) *Molecular Cloning: A Laboratory Manual*. Cold Spring Harbor Laboratory Press, Cold Spring Harbor, NY.
- Scheiffele P & Fullekrug J (2000) Glycosylation and protein transport. *Essays Biochem* **36**: 27–35.
- Smith DJ, Proudfoot A, Friedli L, Klig LS, Paravicini G & Payton MA (1992) PMI40, an intron-containing gene required for early steps in yeast mannosylation. *Mol Cell Biol* **12**: 2924–2930.
- Spiro RG (2002) Protein glycosylation: nature, distribution, enzymatic formation, and disease implications of glycopeptide bonds. *Glycobiology* **12**: 43R–56R.
- Tapon N, Moberg KH & Hariharan IK (2001) The coupling of cell growth to the cell cycle. *Curr Opin Cell Biol* **13**: 731–737.
- Terashima H, Yabuki N, Arisawa M, Hamada K & Kitada K (2000) Up-regulation of genes encoding glycosylphosphatidylinositol (GPI)-attached proteins in response to cell wall damage caused by disruption of FKS1 in *Saccharomyces cerevisiae*. *Mol Gen Genet* **264**: 64–74.
- Travers KJ, Patil CK, Wodicka L, Lockhart DJ, Weissman JS & Walter P (2000) Functional and genomic analyses reveal an essential coordination between the unfolded protein response and ER-associated degradation. *Cell* **101**: 249–258.
- Trotter EW, Berenfeld L, Krause SA, Petsko GA & Gray JV (2001) Protein misfolding and temperature up-shift cause G1 arrest via a common mechanism dependent on heat shock factor in *Saccharomyces cerevisiae*. *Proc Natl Acad Sci USA* **98**: 7313–7318.
- Warner JR (1999) The economics of ribosome biosynthesis in yeast. *Trends Biochem Sci* **24**: 437–440.
- Watanabe I, Zhu J, Recio-Pinto E & Thornhill WB (2004) Glycosylation affects the protein stability and cell surface expression of Kv1.4 but Not Kv1.1 potassium channels. A pore

region determinant dictates the effect of glycosylation on trafficking. *J Biol Chem* **279**: 8879–8885.

Yale J & Bohnert HJ (2001) Transcript expression in *Saccharomyces cerevisiae* at high salinity. *J Biol Chem* **276**: 15996–16007.

Yeong FM, Lim HH, Wang Y & Surana U (2001) Early expressed Clb proteins allow accumulation of mitotic cyclin by inactivating proteolytic machinery during S phase. *Mol Cell Biol* **21**: 5071–5081.

Supplementary material

The following supplementary material is available online:

Fig. S1. Genes differentially expressed in the *pmi40-101* mutant involved in the UPR, protein glycosylation and cell cycle progression pathways. Heat map without cluster analysis showing differential expression of genes for the six trials of the DNA microarray analysis. As shown in the scale bar, red indicates degree of differential induction, and green indicates degree of differential repression. The Fold Change refers to the average of all six experiments, with the indicated *P*-value shown. Function refers to gene descriptions from the *Saccharomyces* Genome database (<http://www.yeastgenome.org>).

Fig. S2. Overlap between the ESR and glycosylation mutant expression profiles. (a) Expression profile of genes differentially expressed >2-fold in the *pmi40-101* mutant (left two panels), and expression profile of known genes induced in the ESR (right panel). The description of the heat map produced for the microarray analysis is as in Fig. S1. (b) Venn diagram illustrating the degree of overlap between the two profiles.

Fig. S3. Nutritionally controlled genes are differentially expressed in the *pmi40-101* mutant. Genes are clustered loosely by function. The description of the heat map produced for the microarray analysis is as in Fig. S1.

Fig. S4. PKC, *fks1* and cell wall genes are differentially expressed in the *pmi40-101* mutant. For the PKC pathway targets, the *CTT1*, *SPS100*, *MLP1*, *PGK1* and *PIR1* profiles are not shown because they contained high *P*-values. The description of the heat map produced for the microarray analysis is as in Fig. S1.

Fig. S5. Genes differentially expressed in the *pmi40-101* mutant that comprise known filamentous growth and HOG pathway targets. The description of the heat map produced for the microarray analysis is as in Fig. S1.

This material is available as part of the online article from <http://www.blackwell-synergy.com>

Author Query Form

Journal **FEMSYR**

Article **120**

Dear Author,

During the copy-editing of your paper, the following queries arose. Please respond to these by marking up your proofs with the necessary changes/additions. Please write your answers clearly on the query sheet if there is insufficient space on the page proofs. If returning the proof by fax do not write too close to the paper's edge. Please remember that illegible mark-ups may delay publication.

Query No.	Description	Author Response
Q1	AQ: Please provide telephone and fax numbers for the corresponding author.	
Q2	AQ: Please check change of Rose (1990) to Rose et al. (1990) is OK.	
Q3	AQ: Please check change of Sambrook (1989) to Sambrook et al. (1989) is OK.	
Q4	AQ: 'Cat8, which encodes a transcription factor for gluconeogenesis (supplementary Fig. S3) and the Cat8 targets' – you give 'Cat8' as a protein (roman type), and then say that it 'encodes' – please clarify.	
Q5	AQ: Lecca, M.R., Wagner, U., Patrignani, A., Berger, E.G., and Hennet, T. (2004). Please supply volume number and page range.	
Q6	AQ: Pitkanen, J.P., Torma, A., Alff, S., Huopaniemi, L., Mattila, P., and Renkonen, R. (2004). Please supply volume number and page range.	
Q7	AQ: Please supply legend for Table 2.	
Q8	AQ: Please supply legend for Table 3.	